08

Effect of morphology, structure and chemical composition on gas-sensing response of thermally modified $Fe_2O_3/Co_xO_y/NiO$ composites

© D.V. Sokolov[1], S.N. Nesov[1], Yu.A. Stenkin[1], V.V. Bolotov[1], K.E. Ivlev[1], I.V. Muromtsev[2]

[1] Omsk Scientific Center, Siberian Branch, Russian Academy of Sciences, Omsk, Russia
[2] Center for New Chemical Technologies at the Institute of Catalysis SB RAS, Omsk, Russia

E-mail: classicsub-zero@mail.ru

Received April 30, 2025
Revised September 8, 2025
Accepted November 11, 2025

Composites of $Fe_2O_3/Co_xO_y/NiO$ were prepared by thermal decomposition with next annealing to modify the morphology, structure and chemical composition. With increasing annealing temperature, the average particle size was increased from 0.11 to 1.00 μm, and the CoO/NiO ratios concentration and Fe, Co, and Ni-containing spinels were changed. Selectivity of the obtained composites to saturated mercury vapor, 500 ppm H_2S and SO_2 at room temperature was demonstrated by a gas sensing study to inorganic gases and organic vapors at various heat treatment temperatures of samples.

Keywords: transition metal oxides, heat treatment, gas response, mercury vapor.

DOI: 10.61011/PSS.2025.12.63097.8002k-25

Mixed transition metal oxides are relevant for gas sensors with controlled selectivity to toxic and flammable gases. The most promising are iron, cobalt and nickel oxides, which have high catalytic activity in the adsorption of Volatile Organic Compounds (VOC) [1], which makes it possible to increase the final sensitivity to certain gases when added to other sensing materials [2–4]. Previous studies of similar multicomponent oxide systems of the composition $Co_{1-x}Ni_xFe_2O_4$ [1], $Co_{1-2x}Ni_xMn_xFe_{2-y}Ce_yO_4$ [5] and $Ni_xCo_{3-x}O_4$ [6] showed sensitivity to various gases at increased temperatures, and systems containing Co_3O_4 oxide also show sensitivity to mercury vapor [7].

Heat treatment (HT) makes it possible to modify the composition and structure of oxide systems, which makes it possible to increase their gas sensitivity and selectivity. Among the oxides of Fe, Co, Ni, reversible transitions occur only in cobalt oxide between CoO and Co_3O_4 during heat treatment above 600 °C [8–10]:

$$6CoO + O_2 \leftrightarrow 2Co_3O_4 \quad (1)$$

When heated to 905−925 °C, cobalt oxide decomposes [8–10]:

$$2Co_3O_4 \rightarrow 6CoO + O_2 \quad (2)$$

These cobalt oxides have different electrical conductivity at gas adsorption, and hence gas sensitivity. Therefore, by adjusting the annealing temperature, it is possible to obtain a certain ratio of Co_3O_4/CoO oxides with the enhanced sensitivity and selectivity. This paper presents the results of a study of the morphology, structure, and sensitivity to inorganic and organic gases at room temperature for composites of the composition $Fe_2O_3/Co_xO_y/NiO$ after heat treatment at 650, 920 and 1000 °C.

Oxide composites were obtained on polycrystalline glass by thermal decomposition of a mixture of saturated solutions of iron, cobalt, and nickel nitrates in a mass ratio of 1:1:1 at 120 °C in air for 120 min to evaporate water. For three series of samples, HT was carried out in air for 60 min at the following temperatures: 650, 920, and 1000 °C.

The morphology of the composites was studied using a JEOL JSM-6610 LV scanning electron microscope (SEM) by an energy dispersive X-ray spectroscopy (EDX) Inca-X-act analyzer to determine the concentration of elements. The crystal structure of the samples was identified based on the results of X-ray diffraction analysis (XRD) on a D8 Advance (Bruker) diffractometer with radiation Cu Kα (wavelength 0.154 nm) in the range of angles 2θ from 5° up to 80°. The chemical composition of the composites was determined by X-ray photoelectron spectroscopy (XPS) at the Surface Science Center (Riber) using non-monochromatic radiation Al Kα (photon energy $\sim$ 1487 eV).

The longitudinal current-voltage characteristics (*I-V* curve) of the composites were measured using an Agilent E4980A precision LCR Meter with a 2 mm distance between two gold-plated contacts. The gas sensing response S was determined at room temperature (19−20 °C) from the resistance changes of the sample in the flow of the following analyzed gases with a concentration of 500 ppm: nitrogen dioxide (NO_2), ammonia (NH_3), hydrazine (N_2H_2), hydrogen (H_2), hydrogen sulfide (H_2S), sulfur dioxide (SO_2); and vapor of ethanol (C_2H_5OH), benzene (C_6H_6), phenol (C_6H_6OH), formic acid (HCOOH), formaldehyde

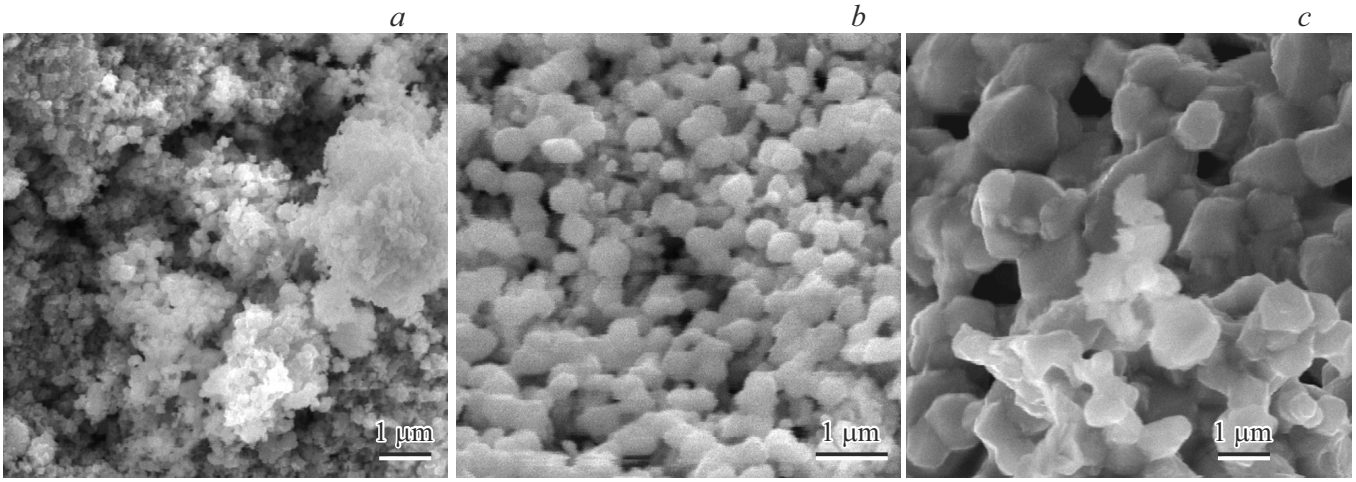

Figure 1. SEM images of composites $Fe_2O_3/Co_xO_y/NiO$ with different HT temperatures: 650 °C (*a*), 920 °C (*b*) and 1000 °C (*c*).

Quantitative elemental composition analysis results for $Fe_2O_3/Co_xO_y/NiO$ at different HT temperatures

Method	HT, °C	Concentration, at.%			
		Fe	Co	Ni	O
EDX	650	10.0	23.0	26.0	41.0
	920	11.8	21.4	24.0	42.8
	1000	7.6	26.3	24.5	41.6
XPS	650	2.0	8.4	27.7	61.9
	920	3.8	15.0	10.5	70.7
	1000	1.8	15.9	15.1	67.2

(HCHO), acetaldehyde (CH_3COH), acetone (CH_3COCH_3) and acetonitrile (CH_3CN). Longitudinal resistance was registered in a closed cell with a volume of 250 ml in a dry nitrogen flow with the analyzed gas (flow rate 0.5–1.0 ml/s, relative humidity 5–8 %) by a ZT219 digital device. For gaseous mercury adsorption study the samples were placed in a cell with saturated Hg vapors. The gas response value was determined as $S = \mathrm{sgn}(R - R_0) \cdot (R/R_0)^{\mathrm{sgn}(R-R_0)}$, where R_0 and R is the stable resistance of the sample before and after gas injection, respectively, $\mathrm{sgn}(R - R_0) = \pm 1$, if R more/less R_0.

The surface of $Fe_2O_3/Co_xO_y/NiO$ composites has a porous granular structure with an average grain diameter of 0.11 ± 0.02, 0.35 ± 0.04 and $1.00 \pm 0.30\,\mu$m for HT at 650, 920 and 1000 °C, respectively (Figure 1). Since cobalt oxide Co_3O_4 decomposes at temperatures 920 °C according to (2), a growth of grain size with increase of HT temperature [10] may be accompanied by an increase in the CoO proportion [9]. According to EDX data, the concentration of elements in composites with different HT weakly varies within the error range of this method (Table).

From the X-ray diffraction analysis results (Figure 2, *a*), crystalline oxides are present in the volume of composites as the following phases: rhombohedral NiO, cubic CoO, cubic spinel of nickel cobaltite $NiCo_2O_4$ and cubic spinel of nickel ferrite (trevorite) $NiFe_2O_4$. The reflexes of NiO oxide are identify only on the X-ray pattern of a sample with HT at 650 °C, and at higher temperatures this oxide forms compounds with Co_2O_3 and Fe_2O_3 oxides. The Fe_2O_3 binds to NiO oxide after HT at 650 °C to form $NiFe_2O_4$, the reflexes of which are also observed on X-ray patterns of samples with higher HT temperature. The CoO oxide reflexes are identified only on X-ray patterns of samples with HT at 920 and 1000 °C.

The intensity of (311), (222), (220) and (200) CoO reflexes on X-ray patterns of samples with HT temperatures 920 °C and higher is increased (Figure 2, *a*). Cobalt oxide Co^{3+} is only in the $NiCo_2O_4$ phase, as indicated by the presence of reflexes (111), (220), (311). Absence of the $NiCo_2O_4$ phase diffraction peaks with reflexes (222), (400), (440), (422) and (511) for HT at 920 °C and 1000 °C may be related to decreasing the polycrystalline grain size and increasing the amorphization degree. Thus, in the $Fe_2O_3/Co_xO_y/NiO$ volume after high-temperature HT, CoO predominates and the Co_3O_4 concentration decreases, which corresponds to reactions (1) and (2).

In the survey XPS spectra of composites, with increase of HT temperature, there is a noticeable decrease in the relative intensity of nickel lines (Figure 2, *b*), which confirms a reduce in its concentration. The position and shape of the Ni $2p$ line corresponds to the charge state Ni^{2+}, which indicates the presence of NiO oxide and $NiCo_2O_4$, $NiFe_2O_4$ spinels in the surface layer of all samples.

The maximum position and the shape of the Co $2p$ spectrum for composite after HT at 650 °C may correspond to the Co^{3+} state, which, in addition with the

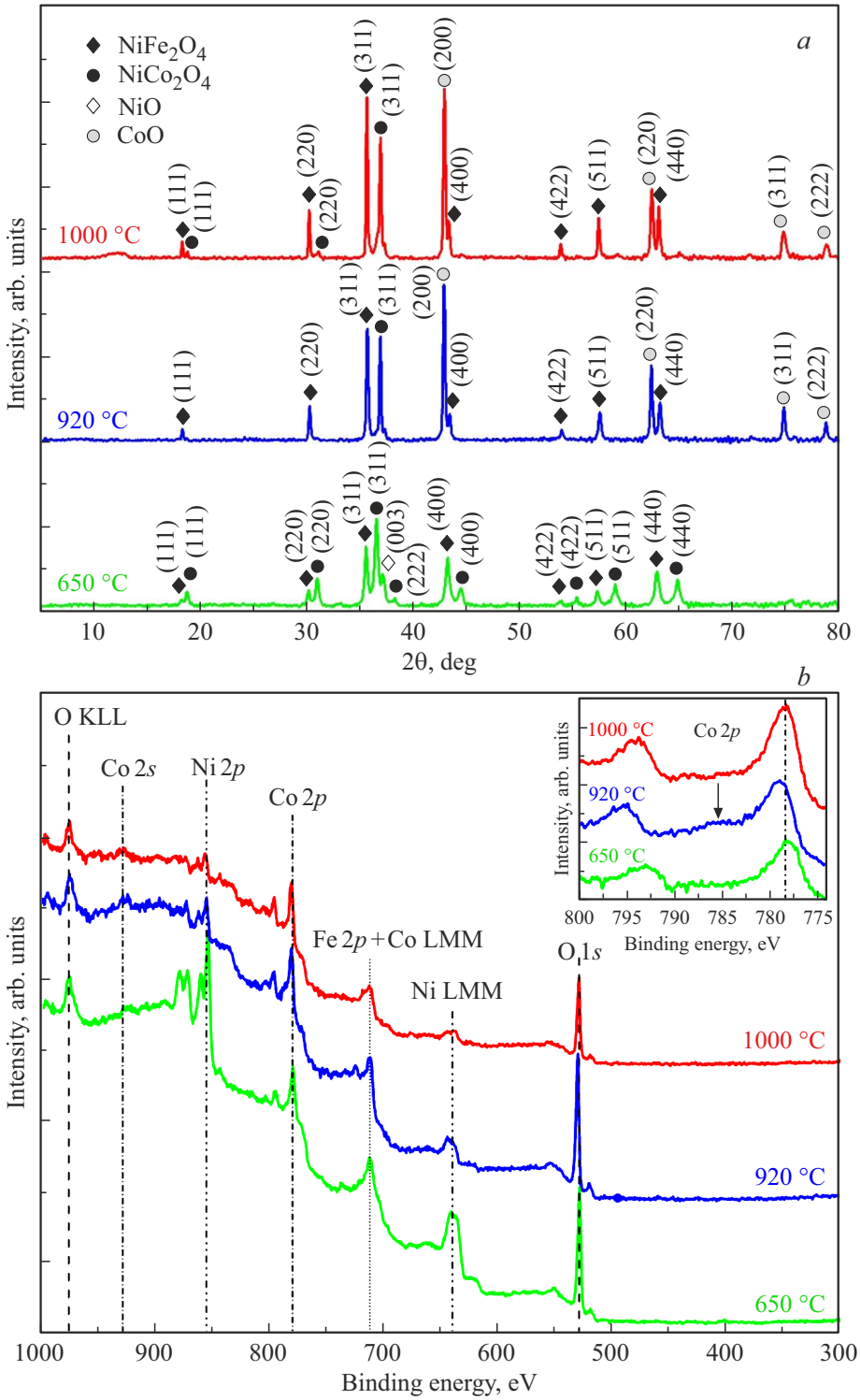

Figure 2. Results of analysis of the structure and composition of samples $Fe_2O_3/Co_xO_y/NiO$ after HT at various temperatures: *a* — X-ray spectra; *b* — survey XPS spectra (the insert shows the spectra of Co 2*p*).

X-ray diffraction data, corresponds to the $NiCo_2O_4$ spinel (Figure 2, *b*, insert). For the Co 2*p* spectrum of the sample with HT at 920 °C a shift of the maximum to the region of low binding energies is observed, as well as a characteristic satellite (indicated by an arrow in the figure), which indicates the presence of Co^{2+} states. This confirms the CoO oxide formation according to the reaction (2). The Co 2*p* spectrum shape of the composite after HT at 1000 °C allows the presence of Co^{2+} and Co^{3+} state to be identified [11]. This may be due to the partial cobalt

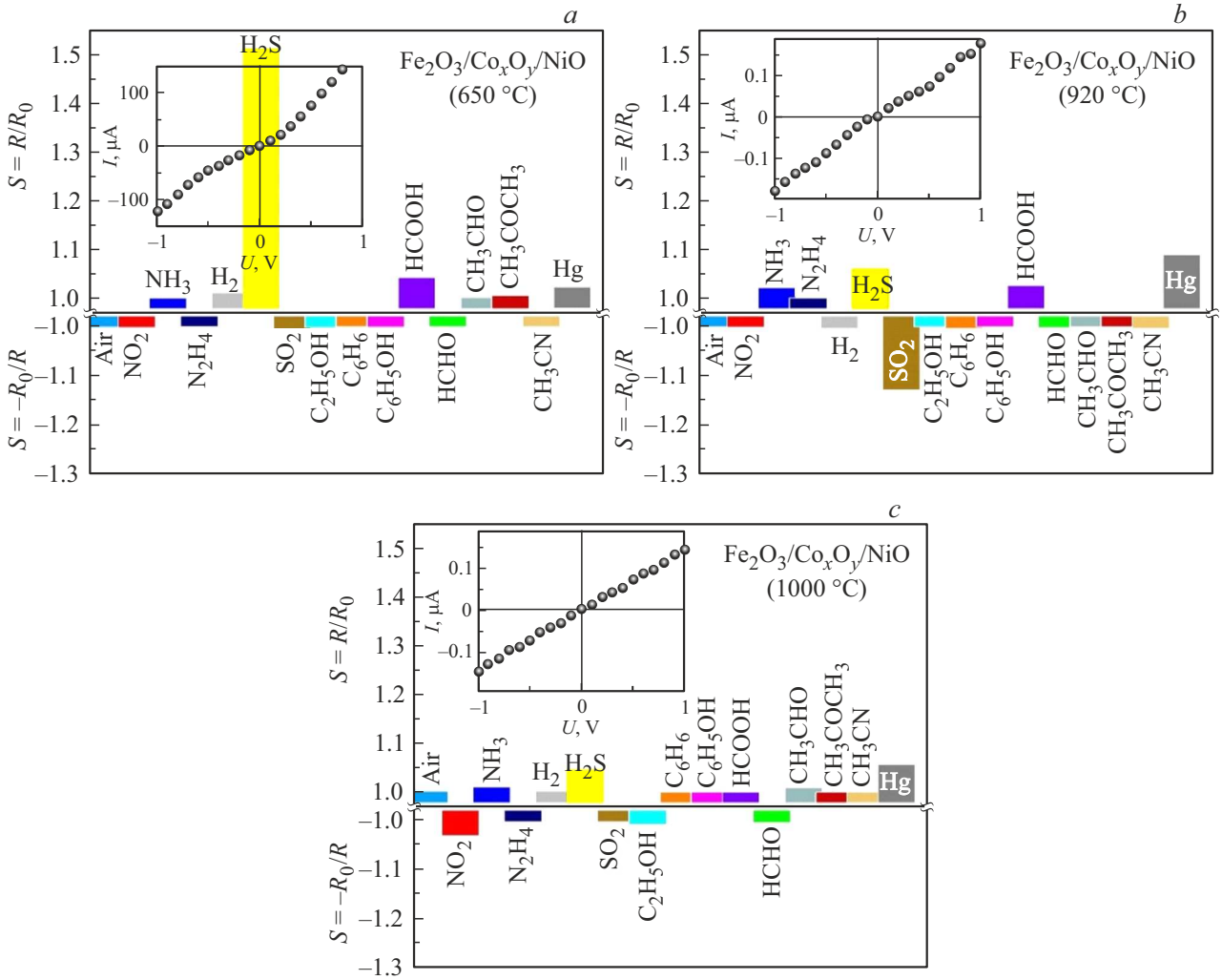

Figure 3. The gas response diagrams of $Fe_2O_3/Co_xO_y/NiO$ composites with different HT temperatures: 650 °C (*a*), 920 °C (*b*) and 1000 °C (*c*); the inserts - corresponding *I-V* curves.

oxidation ($Co^{2+} \rightarrow Co^{3+}$) due to reaction with adsorbed oxygen according to the reaction (1).

The results of quantitative elemental analysis according to the XPS data (Table) demonstrate a significant difference in the elements concentration of the composites surface layer with various HT temperatures. For the samples after HT at 920 and 1000 °C, there is a decrease in nickel concentration (by 1.8 and 2.6 times, respectively) and an increase in cobalt concentration (by 1.8 and 1.9 times, respectively) relative to the sample after HT at 650 °C. The quantitative elemental analysis difference between EDX and XPS (Table) related to the signal detecting depth, which is several micrometers and nanometers, respectively.

The *I-V* curves for $Fe_2O_3/Co_xO_y/NiO$ composites are almost linear (Figure 3, insets). The weakly nonlinear *I-V* curve for composite after HT at 650 °C indicates the possible tunneling of free charge carriers through energy barriers between the oxide components, as well as between conductive contacts and the sample surface. The longitudinal resistance of the $Fe_2O_3/Co_xO_y/NiO$ samples averages 8.45, $6.25 \cdot 10^3$ and $7.10 \cdot 10^3$ kΩ after HT at 650, 920 and 1000 °C, respectively. Due to the presence of high-resistance phases Fe_2O_3 and NiO, the total resistance will be determined by current into conductive Co_xO_y through energy barriers in heterojunctions between oxides [12].

The gas response diagram indicates the *p*-type conductivity of composites — a decrease in resistance for all samples under typical oxidizing gas (NO_2) exposure is observed (Figure 3), while adsorption of typical reducing gases (NH_3, H_2S) leads to an increase in the resistance [1,6].

The composite after HT at 650 °C has significant selectivity to H_2S ($S \approx 1.50$), which corresponds to the results of other studies [3,10]. The response to other gases for this composite is no more than 1.05. For the composite after HT at 920 °C, the response to H_2S decreases to 1.06, and the response to SO_2, on the contrary, increases from 1.01 to 1.13. It is worth noting that this composite has the highest response to Hg vapor ($S \approx 1.09$). Heat treatment at 1000 °C does not lead to a noticeable improvement in the sensing characteristics of the composite: the overall

sensitivity to all gases is noticeably reduced, and the maximum gas response does not exceed 1.06. The likely change of sensitivity is due to a grain size increase and a Co^{2+}/Co^{3+} ratio change.

The mechanism of sensitivity to H_2S at room temperature can occur through the reaction of gas molecules with adsorbed oxygen forms O_2^- during the following reaction [3]:

$$2H_2S_{(ads)} + 3O^-_{2(adc)} \rightarrow 2SO_{2(ads)} + 2H_2O + 3e^-. \quad (3)$$

The high concentration of formed electrons compensates the main charge carriers in composites (holes) [3,4], resulting in a significant increase of the composites resistance compared to the other gases adsorption. The maximum response to H_2S for the composite after HT at 650 °C may be associated with the highest NiO concentration, according to the results of XRD and XPS (Figure 2, Table), which can act as a reaction catalyst (3). In addition, this composite contains grains of the smallest size, which means it has a more high surface area.

During mercury vapor adsorption, the resistance of composites increases due to electron diffusion in the surface layer of the sample ($Hg^0 \rightarrow Hg^{2+} + 2e^-$) and their further recombination with holes. The decrease in the resistance of composites in case of SO_2 adsorption can be explained by reactions in which electrons are captured from the sample surface layer, forming a space charge region enriched in holes [1,5]. As a result, the resistance of the composite with *p*-type conductivity decreases. The catalyst for such reactions may be CoO formed after heat treatment at temperatures above 920 °C. The enhanced response to SO_2 and mercury vapors for the composite after HT at 920 °C is probably achieved by meeting optimal conditions for adsorption — average granule sizes (three times smaller than the composite after HT at 1000 °C) and a sufficient amount of CoO (Figure 2, Table).

The effect of HT temperature on the morphology, structure, chemical composition, and gas sensing properties of a system with the composition $Fe_2O_3/Co_xO_y/NiO$ has been studied. It was found that the nature of the change in gas sensitivity at room temperature is determined by the grain size, the ratio of Co^{2+} and Co^{3+} oxides and the nickel concentration on the grain surface.

It has been shown that in case of HT at 650 °C it is possible to obtain a structure with enhanced gas response to H_2S due to the high concentration of NiO, $NiCo_2O_4$ and $NiFe_2O_4$ in the surface layer, acting as a catalyst for the decomposition of hydrogen sulfide. An increase in gas response to SO_2 and mercury vapor for the composite after HT at 920 °C is ensured by the optimal granule size, as well as a sufficient amount of CoO, which determines the change in the composites conductivity during the adsorption of these gases. The weak sensitivity of the composite after HT at 1000 °C is associated with a decrease in the specific surface area due to an increase in grain size. The results presented in this paper can be used in the development of sensor materials with improved selectivity at room temperature.

Acknowledgments

The study was carried out using the equipment of the Omsk Regional Center for Collective Use of the Siberian Branch of the Russian Academy of Sciences.

Funding

The work was performed under the state assignment of the Omsk Scientific Center SB RAS (state registration number 121021600004-7).

Conflict of interest

The authors declare that they have no conflict of interest.

References

[1] S. Joshi, V.B. Kamble, M. Kumar, A.M. Umarji, G. Srivastava. J. Alloys Compd. **654**, 460 (2016). DOI: 10.1016/j.jallcom.2015.09.119.

[2] V. Bagul, G. Bhagure, B. Langi, D. Tayde. Chem. Rev. Lett. **7**, 433 (2024). DOI: 10.22034/crl.2024.447531.1307.

[3] L. Liu, M. Yang, S. Gao, X. Zhang, X. Cheng, Y. Xu, H. Zhao, L. Huo, Z. Major. ACS Appl. Nano Mater. **2**, 5409 (2019). DOI: 10.1021/acsanm.9b01038.

[4] S. Moon, N.M. Vuong, D. Lee, D. Kim, H. Lee, D. Kim, S.-K. Hong, S.-G. Yoon. Sens. Actuators B: Chem. **222**, 166 (2016). DOI: 10.1016/j.snb.2015.08.072.

[5] S.A. Ogundipe, C.L. Ndlangamandla, M.M. Diale, M. Jozela, H.C. Swart, D.E. Motaung, S.S. Nkosi. Coatings 2023, **13**, 1771. DOI: 10.20944/preprints202308.2198.v1.

[6] M. Govindhan, B. Sidhureddy, A. Chen. ACS Appl. Nano Mater. **1**, 6005 (2018). DOI: 10.1021/acsanm.8b00835.

[7] Z. Liu, X. Xia, H.-K. Guan, Q. Liu, S.-S. Zhao, X.L. Cheng, Q.Q. Xu, S.S. Li. Chem. Eng. J. 435, **2**, 134950 (2022). DOI: 10.1016/j.cej.2022.134950.

[8] R.A. Lidin, V.A. Molochko, L.L. Andreeva. Himicheskie svojstva neorganicheskih veshchestv: ucheb, posobie. INFRA-M, M. (2019). p. 426 (in Russian).

[9] L.J. Cardenas-Flechas, P.T.C. Freire, E.C. Paris, L.C. Moreno, M.R. Joya. Materialia **18**, 101155 (2021). DOI: 10.1016/j.mtla.2021.101155.

[10] T.L. Simonenko, N.P. Simonenko, A.S. Mokrushin, P.Y. Gorobtsov, I.S. Vlasov, I.A. Volkov, E.P. Simonenko, N.T. Kuznetsov. Chemosensors **11**, *3*, 166 (2023). DOI: 10.3390/chemosensors11030166.

[11] Table of Elements. X-ray photoelectron spectroscopy of atomic elements. https://www.xpsfitting.com/2012/01/cobalt.html (accessed 2025).

[12] L. Wang, B. Hong, H.D. Chen, J.C. Xu, Y.B. Han, H.X. Jin, D.F. Jin, X.L. Peng, H.L. Ge, X.Q. Wang. J. Mater. Chem. C **8**, 3855 (2020). DOI: 10.1039/c9tc06614d.

Translated by A.Akhtyamov